THE JOURNAL OF PHYSICAL CHEMISTRY B

Article

pubs.acs.org/JPCB

Multiple Scale Dynamics in Proteins Probed at Multiple Time Scales through Fluctuations of NMR Chemical Shifts

Paolo Calligari*,† and Daniel Abergel*,‡

†International School for Advanced Studies-SISSA/ISAS, via Bonomea 265, 34136 Trieste, Italy

‡Ecole Normale Supérieure, Département de Chimie, UMR 7203 CNRS-UPMC-ENS, 24, rue Lhomond, 75005 Paris, France

ABSTRACT: Fluctuations of NMR resonance frequency shifts and their relation with protein exchanging conformations are usually analyzed in terms of simple two-site jump processes. However, this description is unable to account for the presence of multiple time scale dynamics. In this work, we present an alternative model for the interpretation of the stochastic processes underlying these fluctuations of resonance frequencies. Time correlation functions of ^{15}N amide chemical shifts computed from molecular dynamics simulations (MD) were analyzed in terms of a *transiently* fractional diffusion process. The analysis of MD trajectories spanning dramatically different time scales (~200 ns and 1 ms [Shaw, D. E.; et al. *Science* **2010**, *330*, 341−346]) allowed us to show that our model could capture the multiple scale structure of chemical shift fluctuations. Moreover, the predicted exchange contribution R_{ex} to the NMR transverse relaxation rate is in qualitative agreement with experimental results. These observations suggest that the proposed fractional diffusion model may provide significative improvement to the analysis of NMR dispersion experiments.

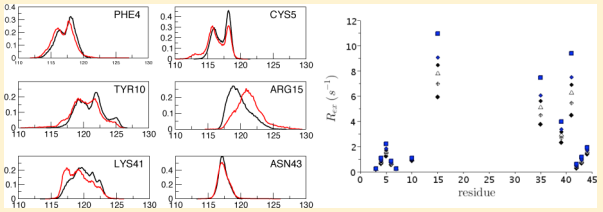

INTRODUCTION

Internal motions in proteins, in addition to the role played by three-dimensional structures, has emerged as an essential factor of such biological functions as enzymatic catalysis, folding, or ligand binding.[1−3] Dynamic processes taking place at the pico- to millisecond time scales are commonly probed by the measurement of spin relaxation by nuclear magnetic resonance (NMR) spectroscopy,[4] and fast, subnanosecond backbone and side chain dynamics in proteins can be investigated through the analysis of T_1, T_2, and NOE relaxation, as well as interference relaxation rates.[5] Alternatively, T_2 relaxation dispersion and $T_{1\rho}$ spin-lock experiments provide a unique approach to probe internal dynamics at the microsecond to millisecond time scales.[6] The latter methods are able to reveal the presence of exchanging conformations, and therefore to monitor the relaxation effects of resonance frequency fluctuations caused by internal motions. The details of the relationship between them cannot be inferred from the sole experiments but a better understanding can in principle be expected from a combination of MD simulations, which give direct access to molecular motions, and of chemical shift calculations.[7] Regarding the latter, a variety of more or less empirical methods have been developed in the past decades to compute chemical shifts of backbone and side chain nuclei, based on sequence alignments against chemical shift databases,[8−11] or on DFT chemical shift calculations using the molecular structure.[12−14] These studies have led to various strategies that are implemented in different software packages made available to the NMR spectroscopist.

Dynamic processes occurring at time scales in the supra-microsecond range are in general not accessible through MD simulations. However, in a notable effort to overcome this barrier, Shaw et al. have built a computer designed to achieve such long time scales[15] and have been able to obtain MD trajectories of small proteins up to 1 ms.[16] These extremely promising results open new avenues for the detailed investigation of rare conformational events with long characteristic times. Such computations have been recently combined with chemical shift calculations in an attempt to rationalize the experimental exchange contributions to NMR transverse relaxation.[17] In this paper, we investigate the stochastic properties of the fluctuations of the nuclei frequencies at a more fundamental level. We present a combined analysis of chemical shift trajectories computed from a 1 ms MD trajectory of the small protein BPTI,[16] together with a short 200 ns simulation of the same protein performed by us in similar conditions. Chemical shift correlation functions computed from these trajectories are analyzed in terms of a *transiently* fractional diffusion process. We show that, when quality permits, data are consistent with a variable order fractional diffusion equation.[18] Moreover, in these favorable cases, similar fractional orders are found in both simulations. This suggests that in spite of the dramatically different sampling rates (2 ps and 25 ns) and lengths (200 ns and 1 ms), the same fractional structure of stochastic process underlying the chemical shift fluctuations can be identified. Such processes imply a distribution of time scales, as typically occurs in complex systems,[19] and associated with a power law decay of the correlation function. However, this kind of decay occurs at intermediate rather than asymptotically long

Received: December 11, 2013
Revised: March 12, 2014
Published: March 14, 2014

   dx.doi.org/10.1021/jp412125d | *J. Phys. Chem. B* 2014, 118, 3823−3831

times, while during the latter, the correlation function decays exponentially to zero. Our analysis of the chemical shift correlation functions performed on the trajectories with the chemical shift as the stochastic variable, strongly suggests the presence of this type of processes.

Finally, based on the simple model of variable order fractional diffusion equation introduced in this work, an analytical expression of the exchange rate R_{ex} is presented and discussed.

METHODS

MD Simulation. We performed all stages of the simulation of BPTI using the GROMACS MD simulation software. The protein structure was taken from the PDB structure 5PTI. The system to be simulated was built by first replacing deuterium atoms with hydrogens and adding 6 chloride ions and 4387 water molecules in a cubic periodic box with a side length of 52 Å. We used the AMBER ff99SB-ildn force field[20] to model all the interaction involving the protein atoms whereas the water was modeled by four-particle TIP4P-Ew force field.[21] Along all the stages of the simulation the LINCS algorithm was used to constraint all bonds involving hydrogen atoms. The resulting structure was minimized to remove possible clashes. System equilibration was performed in two steps. First, to allow for correct relaxation of the water molecule around the protein, the system was equilibrated over 50 000 steps (100 ps) in a *NVT* ensemble using positional restraints to all the protein atoms. Temperature control was achieved by a modified Berendsen thermostat with a 0.1 ps relaxation time.[22] Second, further equilibration was performed for an additional 250 000 steps (1 ns) at constant pressure, keeping the pressure at 1 atm by a Parrinello−Rahman barostat with relaxation time of 2 ps.[23] We used a 10.4 Å cutoff radius for range-limited interactions, with particle mesh Ewald electrostatics evaluated every fifth step using a fifth-order spline interpolation on an FFT grid with maximum spacing equal to 0.16 nm. We extracted the configuration the volume of which was closest to the average volume in this short simulation, which resulted in a cubic box with side lengths of 51.95 Å. For the production run, the simulation box size was kept constant, and the simulation temperature was controlled by the modified Berendsen thermostat. The simulation time step was 2 fs, with long-range electrostatics evaluated every other time step.

Chemical Shifts Calculations. Each frame of both the 1 ms and 200 ns trajectories was dumped into a pdb file and then submitted to the SHIFTX2 software (Version 1.07)[11] for the prediction of backbone ^{15}N chemical shifts, using a temperature of 298 K and pH 5 as optional arguments. The obtained time-series of chemical shifts (CS) for each residue were collected for further analysis.

Correlation Functions. The chemical shift correlation functions $C(t)$ were computed from CS time series using customary algorithms[24] and were fitted to eq 27. The cost function $X^2 = [C_I(t) - C_I^{ML}(t)]^2$ was minimized using the so-called bound-constrained "limited memory Broyden−Fletcher−Goldfarb−Shanno" (L-BFGS-B) optimization algorithm.[25]

THEORY

Description of Chemical Exchange with a Variable Order Fractional Diffusion Equation. From the NMR spectroscopist's viewpoint, relating measurements of exchange contributions R_{ex} to chemical shift fluctuations, and therefore to backbone dynamics, is of particular interest. Owing to usual definitions,[26] the contribution R_{ex} to transverse relaxation in conditions of fast exchange is equal to the zero frequency component of the Fourier transform of the resonance frequency correlation function $\Omega(t)$:

$$R_{ex} = \int_0^\infty \Omega(\tau)\, d\tau = \int_0^\infty \langle(\omega(t) - \langle\omega\rangle)\cdot(\omega(t+\tau) - \langle\omega\rangle)\rangle\, d\tau \quad (1)$$

where $\omega(t)$ is the instantaneous resonance frequency of the spin and $\langle\omega\rangle$ its ensemble average, and the process is assumed stationary. Obviously, significant exchange contributions can only originate from slowly decaying correlation functions. Experimentally observed R_{ex} contributions are usually interpreted in terms of Markovian two-state models, although a diffusion model has also been suggested.[27] These are of course idealizations, which are mainly imposed by the scarcity of data and which are probably often unlikely considering the complexity of protein motions, as can be viewed for instance by MD simulations. For instance, in favorable cases, discarding the details of the potential eigenmodes, and representing the latter through a single effective eigenvalue instead, are acceptable.

However, an aspect generally overlooked in this context is the presence of fractional difusional processes, which are characteristic of complex systems. At the microscopic level, it can be interpreted as the presence of energetic obstacles and traps that slow down diffusion. This process can be described by a continuous time random walk (CTRW), where the waiting time probability distribution function has a power law time dependence, leading to a diverging first moment of the waiting time. Therefore, one cannot define a time scale of the random process in this case,[19] which is in contrast to Brownian diffusion.

At a different level of description, this process introduces memory effects[28] that are conveniently described by a fractional diffusion equation.[29] The existence of such processes has been attested in various studies in the literature,[30−32] and suggested by our previous work on protein dynamics based on the analysis of MD simulations.[33−35]

In the present context, this approach provides a way to account for complex, subdiffusive, dynamics associated with asymptotic power law decays of the correlation functions of eq 1. This sort of idealization may lead, however, to certain difficulties, due to the fact that a power law decay of $\Omega(t)$ is associated with a diverging integral in eq 1. This kind of problem was avoided in the study of orientational correlation functions of chemical bonds in proteins.[33−35] In that case, the relevant correlation function was the product of an internal fractional and an overall exponential correlation functions, which ensured a decay of exponential order at $+\infty$ of the correlation function. In contrast, such a regularization does not arise naturally in the present case. However, this issue is circumvented through the use of a variable order fractional diffusion equation with fractional order α that tends to unity at long evolution times.

This further allows the computation of R_{ex} as the Fourier transform of the chemical shift correlation function. Fractional diffusion is in essence an asymptotic theory that originates from the theory of continuous time random walks (CTRW) with power law decay of the waiting time pdf $\psi(t)$.[19,36] It is shown

dx.doi.org/10.1021/jp412125d | J. Phys. Chem. B 2014, 118, 3823−3831

that this process gives rise to a fractional Fokker–Planck equation (FPE):[19]

$$\frac{\partial P(x,t)}{\partial t} = \tau_0^{1-\alpha}\mathcal{D}_t^{1-\alpha}L_{\mathrm{FP}}P(x,t) \tag{2}$$

where

$${}_0\mathcal{D}_t^{1-\alpha}f(t) = \frac{1}{\Gamma(\alpha)}\frac{\mathrm{d}}{\mathrm{d}t}\int_0^t [t-t']^{\alpha-1}f(t')\,\mathrm{d}t' \tag{3}$$

is the fractional differential operator,[37] $\Gamma(\alpha)$ is the Gamma function, L_{FP} is the Fokker–Planck operator, and $0 < \alpha \leq 1$. In the case of fractional diffusion in a harmonic potential, the correlation function $C(t) = \langle x(t)\, x(t+\tau)\rangle$ of eq 2 is the Mittag–Leffler (ML) function, defined as

$$E_\alpha(z) = \sum_{k=0}^{\infty}\frac{z^k}{\Gamma(1+\alpha k)} \tag{4}$$

which is an entire function of the complex argument z.[38] For $0 < \alpha \leq 1$, the stretched ML function can be expressed as the continuous superposition of exponential relaxation functions $\exp(-\lambda t)$, with the relaxation rate distribution function $p_{\alpha,\tau}(\lambda)$:

$$E_\alpha(-[t/\tau]^\alpha) = \int_0^\infty \mathrm{d}\lambda\, p_{\alpha,\tau}(\lambda)\exp(-\lambda t) \tag{5}$$

The spectrum of relaxation rates is positive and has the form[30,39]

$$p_{\alpha,\tau}(\lambda) = \frac{\tau}{\pi}\frac{(\tau\lambda)^{\alpha-1}\sin(\pi\alpha)}{(\tau\lambda)^{2\alpha}+2(\tau\lambda)^\alpha\cos(\pi\alpha)+1} \tag{6}$$

with the normalization condition $\int_0^\infty \mathrm{d}\lambda\, p_{\alpha,\tau}(\lambda) = 1$. The scaling parameter τ is related to the median $\lambda_{1/2}$ of $p_{\alpha,\tau}(\lambda)$ through $\lambda_{1/2} = \tau^{-1}$.[40] For $\alpha = 1$, $p_{\alpha,\tau}(\lambda)$ reduces to a Dirac distribution centered at the value τ^{-1} and $E_1(z) = \exp(z)$, whereas for $0 < \alpha < 1$ it exhibits a power law decay at long times. For a potential of arbitrary shape, eq 2 can be formally solved by using the separation ansatz: $P(x) = \sum_{n=0}^\infty \Phi_n(x)\, T_n(t)$. The decay and spatial modes satisfy the equations[19]

$$\frac{\mathrm{d}}{\mathrm{d}t}T_n(t) = -\lambda_{n,\alpha}\,{}_0D_t^{1-\alpha}T_n(t) \tag{7}$$

$$L\Phi_n(x) = -\lambda_{n,\alpha}\Phi_n(x) \tag{8}$$

where $\lambda_{n,\alpha} = \lambda_n\,\tau^{1-\alpha}$, and λ_n is the nth eigenmode of the Fokker–Plank operator L. The decay modes are thus the ML functions: $T_n(t) = E_\alpha[-\lambda_{n,\alpha}t^\alpha] = E_\alpha[-\lambda_n\tau(t/\tau)^\alpha]$. And the correlation function $C(t)$ is a superposition of ML functions of the various modes:

$$C(t) = \sum_n a_n E_\alpha[-\lambda_n\tau(t/\tau)^\alpha] \tag{9}$$

In favorable cases, the exact correlation function can be approximated by a single ML decay with an effective eigenmode λ_{eff}, so that

$$C(t) \approx E_\alpha[-\lambda_{\mathrm{eff}}\tau(t/\tau)^\alpha] = E_\alpha[-(t/\tau_{\mathrm{eff}})^\alpha] \tag{10}$$

where $\tau_{\mathrm{eff}}^{-\alpha} = \lambda_{\mathrm{eff}}\tau^{1-\alpha}$. A *transiently* fractional diffusion process can be modeled through a *variable order* fractional FPE,[18] where the stochastic process obeys a FFPE ($\alpha < 1$) for early times, whereas for large values of t, eq 2 becomes a conventional FPE, with $\alpha = 1$:

$$\frac{\partial P(x,t)}{\partial t} = \tau(t)_0^{1-\alpha(t)}\mathcal{D}_t^{1-\alpha(t)}L_{\mathrm{FP}}P(x,t) \tag{11}$$

A justification of this apparently ad hoc equation is sketched in the Appendix. Unfortunately, this equation is not in general amenable to an analytical solution. However, the simple case where $(\alpha(t_1), \tau(t_1)) = (\alpha, \tau)$ for t smaller than some threshold time t_c and $(\alpha(t_1), \tau(t_1)) = (1, \tau_c)$ when $t > t_c$, can be easily handled. Equation 11 thus reads

$$\frac{\partial P(x,t)}{\partial t} = \tau^{1-\alpha}[1-\mathcal{U}(t-t_c)]_0\mathcal{D}_t^{1-\alpha}L_{\mathrm{FP}}P(t) + \mathcal{U}(t-t_c)L_{\mathrm{FP}}P(t) \tag{12}$$

where $\mathcal{U}(t)$ denotes the unit step function. For diffusion in a harmonic potential $V(x) = Kx^2/2$, one has[40]

$$L_{\mathrm{FP}} = D\frac{\partial^2}{\partial x^2} + \mu K\frac{\partial}{\partial x}x \tag{13}$$

with $\mu = D/k_{\mathrm{B}}T$. The correlation function $C(t)$ therefore writes

$$\frac{\mathrm{d}C(t)}{\mathrm{d}t} = -[1-\mathcal{U}(t-t_c)]_0\mathcal{D}_t^{1-\alpha}\mu\tau^{1-\alpha}KC(t) - \mathcal{U}(t-t_c)\mu KC(t) \tag{14}$$

$$= -\mu K\{\tau^{1-\alpha}[1-\mathcal{U}(t-t_c)]_0\mathcal{D}_t^{1-\alpha} + \mathcal{U}(t-t_c)\}C(t) \tag{15}$$

Owing to the above definitions, K is related to a time $\tau_c = (\mu K)^{-1}$. The decay time is then redefined as $\tau^{-\alpha} \equiv \tau_c^{-1}\tau^{1-\alpha}$,[33] so that eq 14 becomes

$$\frac{\mathrm{d}C(t)}{\mathrm{d}t} = -\{\tau^{-\alpha}[1-\mathcal{U}(t-t_c)]_0\mathcal{D}_t^{1-\alpha} + \tau_c^{-1}\mathcal{U}(t-t_c)\}C(t) \tag{16}$$

which admits the solution

$$C(t) = [1-\mathcal{U}(t-t_c)]E_\alpha[-(t/\tau)^\alpha] + \mathcal{U}(t-t_c)E_\alpha[-(t_c/\tau)^\alpha]\mathrm{e}^{-(t-t_c)/\tau_c} \tag{17}$$

In eq 17 the value of t_c is assumed to be long enough for $E_\alpha[-(t_c/\tau)^\alpha]$ to be in the power-law regime ($0 < \alpha < 1$) and[36]

$$E_\alpha[-(t_c/\tau)^\alpha] \sim \left(\frac{\tau}{t_c}\right)^\alpha \qquad t_c \gg \tau \tag{18}$$

One may also impose the condition that $C(t)$ is a smooth function for $t > 0$, so that it should have a continuous derivative at the regime transition $t = t_c$:

$$\left[\frac{\mathrm{d}}{\mathrm{d}t}E_\alpha[-(t/\tau)^\alpha]\right]_{t_c} = E_\alpha[-(t_c/\tau)^\alpha]\left[\frac{\mathrm{d}}{\mathrm{d}t}\mathrm{e}^{-(t-t_c)/\tau_c}\right]_{t_c} \tag{19}$$

Assuming equality in eq 18, one finds the constraints

$$\frac{\alpha\tau_c}{t_c} = 1, \qquad t_c \gg \tau \tag{20}$$

Calculation of the Exchange Rate R_{ex}. The model presented here provides an analytical expression of the exchange rate R_{ex}, defined as

$$R_{\mathrm{ex}} = \omega_0{}^2\langle(\delta(t)-\langle\delta\rangle)^2\rangle\int_0^\infty C(t)\mathrm{d}t \tag{21}$$

dx.doi.org/10.1021/jp412125d | J. Phys. Chem. B 2014, 118, 3823–3831

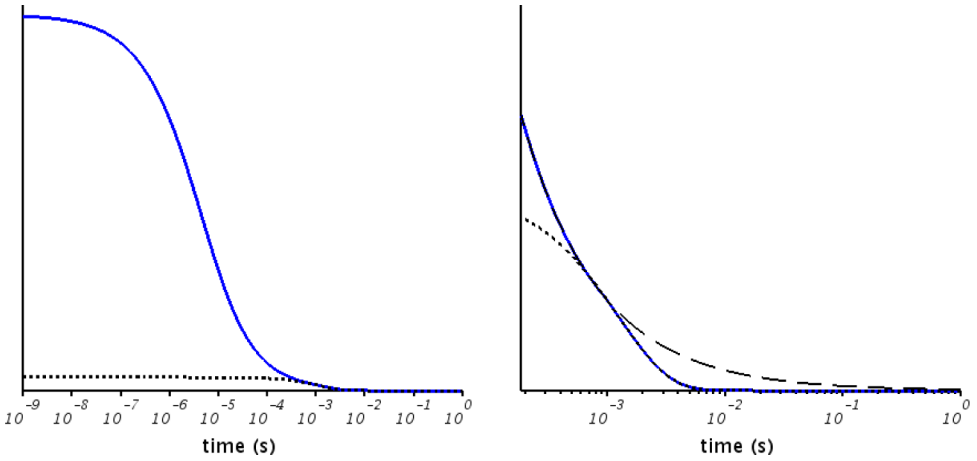

Figure 1. Illustrative example of the Mittag−Leffler to exponential transition in a simple case of transiently fractional diffusion process where $(\alpha(t_1), \tau(t_1)) = (\alpha, \tau)$ for $t < t_c$ and $(\alpha(t_1), \tau(t_1)) = (1, \tau_c)$ when $t > t_c$.The solid lines denote the correlation function. Dashed and dotted lines represent the ML and exponential contributions to $C(t)$, respectively.

where ω_0 is the Larmor frequency for ^{15}N nuclear spins. Using eq 17, this gives

$$R_{ex} = \omega_0^2\langle(\delta(t) - \langle\delta\rangle)^2\rangle\{\int_0^{t_c} c_{el}E_\alpha[-(t/\tau)^\alpha]\,dt + c_{el}E_\alpha[-(t_c/\tau)^\alpha]\int_{t_c}^{\infty} e^{-(t-t_c)/\tau_c}\,dt\} \quad (22)$$

The first term in the rhs can be evaluated using the relation[41]

$$\int_0^z t^{\beta-1}E_{\alpha,\beta}(wt^\alpha)\,dt = z^\beta E_{\alpha,\beta+1}(wz^\alpha) \quad (23)$$

where

$$E_{\alpha,\beta}(z) = \sum_{k=0}^{\infty}\frac{z^k}{\Gamma(\alpha k + \beta)} \quad \text{with } \alpha, \beta \in C,\ \mathrm{Re}(\alpha) > 0,\ \mathrm{Re}(\beta) > 0 \quad (24)$$

is the generalized Mittag−Leffler function and $E_{\alpha,1}(z) = E_\alpha(z)$. In the problem at hand, one may evaluate R_{ex} with the help of eq 20 as

$$R_{ex} = \omega_0^2\langle(\delta(t) - \langle\delta\rangle)^2\rangle c_{el}\{t_cE_{\alpha,2}[-(t_c/\tau)^\alpha] + \tau_cE_\alpha[-(t_c/\tau)^\alpha]\} \quad (25)$$

This expression can be evaluated numerically.[42]

Note that the value of the transition time t_c is likely to have significant impact on R_{ex}. Indeed, the slow $\sim(\tau/t)^\alpha$ evolution of the ML component of the correlation function $C(t)$ is followed by a fast exponential decay (eq 17), and as shown in Figure 1, for $t > t_c$, the area between the ML curve and $C(t)$ diverges, as the former has infinite integral.

Moreover, this influence of t_c on R_{ex} values depends on α, and the closer α is to unity, the steeper the decay of the long time tail and the lesser the effect on R_{ex}.These points will be discussed in the next section.

Practical Model Implementation for MD Simulations Analysis. The analysis of the statistical properties of the chemical shift as a random variable $\delta(t)$ is based on the study of its (normalized) correlation function:

$$C(t) = \frac{\langle(\delta(0) - \langle\delta\rangle)\cdot(\delta(t) - \langle\delta\rangle)\rangle}{\langle(\delta(0) - \langle\delta\rangle)^2\rangle} \quad (26)$$

In this work, $C(t)$ was computed from the sequences of chemical shift values predicted from atomic coordinates sampled by MD simulations at time intervals Δt = 2 ps and Δt = 25 ns for the 200 ns and the 1 ms trajectories, respectively.

Time-averaged correlation functions obtained from MD simulations are used to numerically approximate the ensemble average of eq 26. This approximation is plausible when the largest characteristic time of the system is much shorter than the simulation duration.

Then, as a rule of thumb, correlation functions are considered statistically reliable only for time lags that are at most equal to 10% of the total trajectory length.[43] However, even under these restrictive conditions the approximation may not be satisfied when motions take place at a distribution of time scales, as in the case of such large complex systems as proteins. Some processes may therefore be statistically ill sampled whatever the length of the trajectory, which affects the computation of correlation functions. This can have deleterious effects on fitting, when the value of the correlation function is on the order of the amplitude of these perturbations. Therefore, in some cases, shorter fractions of the correlation functions were used for model fitting.

To get an idea of the way the values of α are affected by the statistical noise of the correlation functions, we compared values obtained by fitting the first 10% and 4% of their total lengths. In the case of the 200 ns simulation, an average relative difference was estimated to be on the order of 5−10%, except for residue 15, for which the relative difference between $\alpha_{4\%}$ and $\alpha_{10\%}$ was around 15%. However, observation reveals an oscillatory-like behavior of the correlation function, strongly suggestive of insufficient averaging. Similar observations were made on the 1 ms trajectory. Finally, this led us to restrict the analysis of the correlation functions to time lags shorter than 4% its total length in the case of the 1 ms trajectory, whereas the usual 10% threshold was retained for our 200 ns simulation.

Moreover, numerical evaluation of correlation functions are affected by the sampling time step. Indeed, the presence of processes with characteristic times shorter than the sampling time leads to an initial steep drop. The latter can be as large as 40−60% of the total decay and is constantly observed on $C(t)$ computed from the sequences of chemical shifts. In a trajectory with a sampling time as short as Δt = 2 ps, this may correspond to dynamics related to chemical bond vibrations and libration.

dx.doi.org/10.1021/jp412125d | J. Phys. Chem. B 2014, 118, 3823−3831

Alternatively, in trajectories sampled with Δt = 25 ns, this may result in a filtering of relaxation times shorter than Δt. In any event, the initial drop of $C(t)$ was taken into account through the additional parameter c_{el}, which acts as a scaling factor in eq 17.[33,34]

The transiently fractional diffusion model discussed in this work assumes that the distribution of decay rates of the correlation function $C(t)$ is bounded by τ_c which, as eq 20 indicates, is on the same order of magnitude as the transition time lag t_c to normal diffusion. Therefore, due to the presence in many cases of noisy $C(t)$ in the 1 ms trajectory, we assumed that the value of t_c was at least larger than the 4% of the trajectory length that was used as the maximum time lag for the computation of the correlation functions. These considerations therefore substantiated the choice to fit the CS correlation functions computed from the MD simulations to the simpler expression:

$$C(t) = c_{el}E_\alpha[-(t/\tau)^\alpha] \quad (27)$$

which left the parameter t_c undetermined.

RESULTS AND DISCUSSION

Correlation Function Analysis. In the 1 ms trajectory, correlation functions exhibiting decays that extended over a significant number of data points were fitted to eq 27. Not surprisingly, the corresponding residues are among those for which an exchange contribution was measured experimentally.[44,45] Overall, the correlation functions corresponding to residues ASP3-TYR10, ARG15, TYR35, ARG39, LYS41, ARG42, ASN43, and ASN44 could be fully analyzed. For these residues reliable fits of the correlation functions to our model were obtained and α, τ, and c_{el} model parameters extracted (Table 1).

Table 1. Fitting Parameters α, τ, and c_{el} of the Model Function $C(t)$ Given in Eq 27 Obtained from the Comparison with Chemical Shift Correlation Functions from the 1 ms MD Trajectory

Res	α	τ (μs)	c_{el}
3	0.94	3.80	0.13
4	0.66	3.11	0.11
5	0.66	2.48	0.23
6	0.73	3.59	0.15
7	0.98	3.79	0.19
10	0.87	2.97	0.22
15	0.64	6.18	0.39
35	0.61	10.00	0.19
39	0.68	2.56	0.37
41	0.59	15.34	0.16
42	0.58	1.57	0.09
43	0.69	5.02	0.25
44	0.80	12.94	0.11

Chemical shifts and their correlation functions were computed also on the 200 ns MD trajectory, which was performed under identical conditions in terms of force field and water model (see Methods). For a number of residues, the range of chemical shifts was satisfactorily explored during this short MD trajectory. This was attested by the excellent superposition of the CS histograms obtained from both trajectories, as illustrated in Figure 2. This of course did not exclude the possibility of chemical shift fluctuations at larger

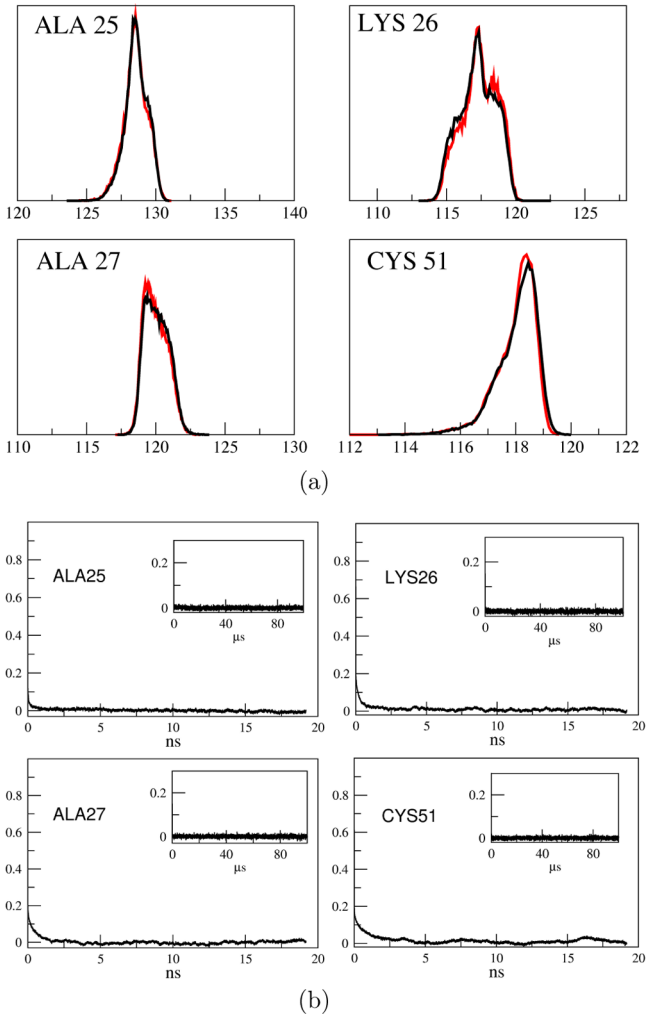

Figure 2. (a) Distribution of chemical shift values from 200 ns (black) and 1 ms (red) trajectories for ALA 25, LYS 26, ALA 27, and CYS 51. (b) Correlation functions $C(t)$ for the residues shown in (a). $C(t)$ from the 1 ms trajectory are displayed in the insets.

time scales than can be satisfactorily sampled during the MD simulation. But in any event, these favorable cases provided correlation functions of better quality and likely to be analyzed.

Moreover, it is worth noting that for most residues, correlation functions could be analyzed only for the 200 ns trajectory, as the decays of their counterparts from the 1 ms MD were complete within the Δt = 25 *ns* sampling used in the simulation (compare Tables 1 and 2). Overall, complete analysis of the 200 ns trajectory data allowed us to satisfactorily fit the correlation functions of residues ASP3-TYR10, ARG15, TYR21, ASN24-GLY28, PHE33, LYS41, ASN43, and CYS51. The resulting model parameters are indicated in Table 2, and examples of residues for which exploitable correlation functions were found in both trajectories are shown in Figure 3.

Residues Cys14 and Cys38 are known to exhibit exchange broadening, resulting from isomerization of the disulfide bridge betwwen them.[44] However, the data at hand did not allow for an analysis of the respective correlation functions, which failed to meet the required quality conditions. Indeed, no clear plateau value was reached within the first 10% of their total length, and these correlation functions even become negative after 25% of the points (Figure 4). This unfavorable behavior was clearly due to intrinsic poor statistics of correlation

dx.doi.org/10.1021/jp412125d | J. Phys. Chem. B 2014, 118, 3823−3831

Table 2. Fitting Parameters α, τ, and c_{el} of the Model Function $C(t)$ Given in Eq 27 Obtained from the Comparison with Chemical Shift Correlation Functions from the 200 ns MD Trajectory

Res	α	τ (ps)	c_{el}
3	0.43	35.05	0.39
4	0.68	87.11	0.22
5	0.62	378.40	0.17
10	0.44	36.17	0.44
15	0.43	2262.80	0.46
21	0.51	56.11	0.22
24	0.43	11.17	0.61
25	0.59	9.16	0.36
26	0.61	56.64	0.34
27	0.77	157.79	0.27
28	0.62	30.40	0.36
33	0.77	245.86	0.22
41	0.46	3.81	0.55
43	0.70	1663.83	0.25
51	0.69	410.46	0.20

functions, likely related to ill sampled rare events in the 1 ms trajectory. Therefore, a comparison with a model function would be highly questionable in this case.

Comparison of the ML Parameters Obtained from Both Simulations. One of the main goals of the present study was to characterize the statistics of the chemical shifts as random variables from MD simulations, and to show the presence of fractional diffusion processes at the time scales probed. In the fractional Brownian diffusion model, as described by the fractional FPE (eq 2), the parameter α appearing in $E_\alpha(-[t/\tau]^\alpha)$ characterizes the nature of the decay of the correlation function and defines the algebraic long time tail decay of the waiting time pdf of the associated random walk process, $\Psi(t) \sim t^{-(1+\alpha)}$.[29] To make a comparative study of the α model parameter meaningful, one must therefore ensure that the chemical shift potentials (the drift term in the FFPE), as probed by the MD simulations, are similar in both cases. This can be verified by comparing the chemical shift distributions obtained from the 200 ns and 1 ms trajectories.

Fast sampling of the CS sets an upper bound to the frequency range probed during the simulation, whereas a relatively short duration of the MD trajectory imposes a limitation on the low frequencies that can be sampled. Therefore, the analyses of CS trajectories at two different sampling rates and durations yield two different pictures through the sampling of different eigenmodes $\lambda_{n,\alpha}$ of the FP operator and provide different values of the effective λ_{eff} in eq 10. But of course, as mentioned in the previous section, the value of α remains unchanged, so that one expects to extract the same values of this parameter from either trajectory. Thus, residues for which chemical shift histograms obtained from both trajectories were considered identical were retained as good candidates for a comparative analysis of the α parameters

This was the case for residues PHE4, CYS5, and ASN43 (Figure 5). For these residues, satisfactory ML fits yielded the same values of α in both trajectories. This very fact strongly suggests that the stochastic processes that are probed by both simulations have the same structure, and that the *same* fractional diffusion process underlies the statistical properties of the CS fluctuations, however dramatically different the sampling rates and observation windows may be. The absence

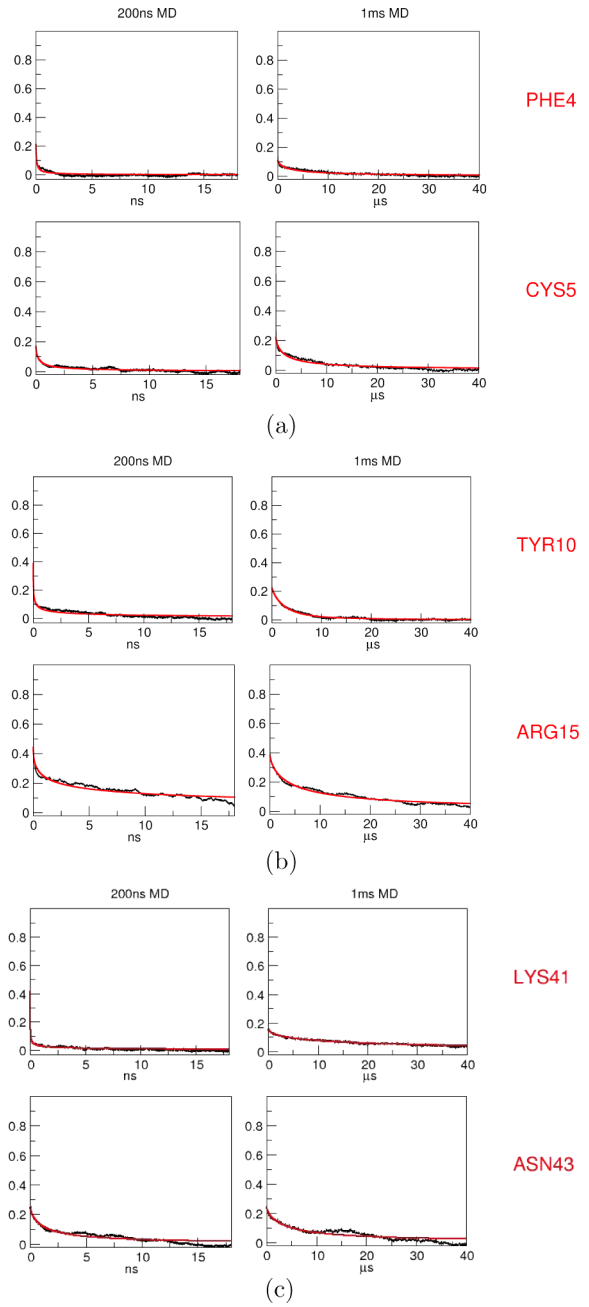

Figure 3. Correlation functions $C(t)$ for residues PHE4, CYS5 (a), TYR10, ARG15 (b), and LYS41, ASN43 (c). The shown $C(t)$ are from 200 ns (left) and 1 ms (right) MD trajectories.

of a time scale for the process illustrates the time fractal character of the correlation function.

In contrast, the same analysis led to clear discrepancies in the case of residues TYR10, ARG15, and LYS41. These could be attributed to the dissimilarity between CS histograms extracted from the 200 ns and 1 ms trajectories (Figure 5), which indicated different apparent effective potentials in each case. Therefore, following the above discussion, α values may not be used in a straightforward manner to characterize the underlying stochastic process and to provide a basis for a comparison of the two trajectories. Thus, asserting the similarities and the differences of chemical shift distributions for a residue in both simulations may not be an easy task. Residues PHE4 and CYS5 shown in Figure 5 seem to exhibit similar doubly peaked

dx.doi.org/10.1021/jp412125d | J. Phys. Chem. B 2014, 118, 3823−3831

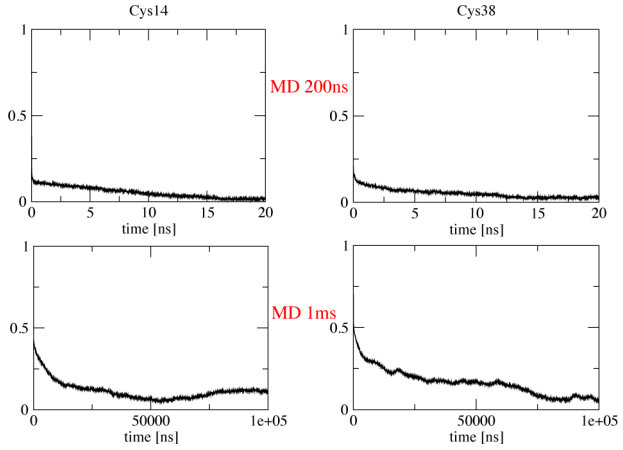

Figure 4. Correlation functions for Cys14 and Cys38.

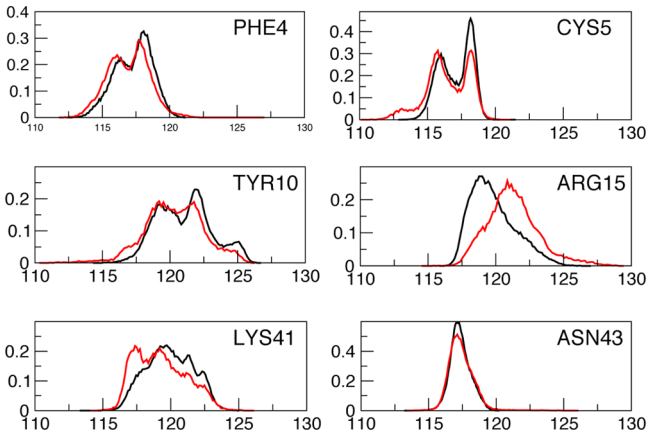

Figure 5. Distribution of chemical shifts values in the 200 ns (black) and 1 ms (red) trajectories. Residues shown are those for which a comparison between the two trajectories can be made.

distributions with the same overall profiles. In contrast, discrepancies are apparent in the case of LYS41, where the chemical shift distributions seem to match for values larger than ca. 118 ppm, whereas clearly a peak around 117 ppm is present only on the 1 ms trajectory. It was possible to go somewhat beyond qualitative statements in the case of residue TYR10. Extracts of increasing lengths of the full 1 ms chemical shift trajectory were selected, and correlation functions were computed and fitted to the fBD model. Interestingly, our results show that, as the length of the excerpt decreases, the distribution approaches its doubly peaked counterpart from the 200 ns simulation (Figure 6). Moreover, the analyses of fragments representing 50%, 10%, and 8% of the 1 ms trajectory yielded decreasing α = 0.80, 0.54, 0.36, reaching values close to α = 0.44, which was obtained from the shorter 200 ns simulation. A similar analysis of LYS41, was not made possible because of too noisy correlation functions obtained from fragments of the total trajectory.

***R_{ex}* Evaluation.** Estimates of the exchange rate R_{ex} can in principle be calculated from the (α, τ, c_{el}) model parameters obtained from the 1 ms CS time sequences. However, as explained above, the cutoff time t_c could not be extracted from the simulations, as in general, much longer trajectories would be necessary to obtain data sets that yield correlation functions with acceptable noise levels even for time lags on the order of tens of microseconds or larger. Under these circumstances, it is

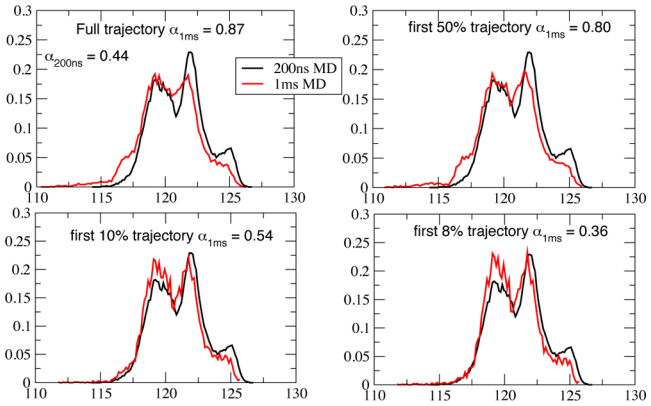

Figure 6. Effect of different sampling of chemical shift fluctuations for Tyr10.

only possible to investigate the influence of t_c on the calculated value of R_{ex}. Thus, exchange rates were calculated with the parameters given in Table 1 for values of t_c ranging from 100 to 500 μs. Results are depicted in Figure 7 and show that the

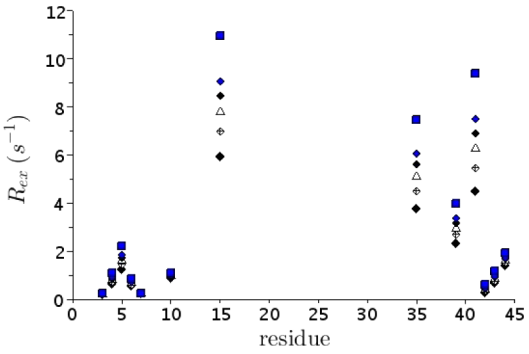

Figure 7. R_{ex} calculated from eq 25 for different values of t_c.

values of R_{ex} increase with increasing t_c. This effect is more pronounced for larger c_{el} and τ, and smaller α, which can be understood from eq 25. This illustrates the dominant contribution to the integral of the power law tail of the correlation function with respect to its exponential asymptotic decay.

It should be noted that, while revealing a pattern of exchange rates that exhibits qualitative agreement with experimental R_{ex} values,[44] comparison is limited due to various sources of error, including the still unsufficient duration of the MD simulation, the lack of accuracy of the chemical shift predictions, and also experimental uncertainties. These points were discussed in ref 17. Note in this respect that numerical integration of the chemical shift correlation functions, hence computed values of R_{ex}, can be achieved irrespective of the model used for the correlation function. In this sense, the comparison between MD and experimental data does not per se constitute a test of the dynamical model, although satisfactory agreement is obviously necessary for a model assessment to be meaningful.

CONCLUSION

In this article, we presented an analysis of chemical shift fluctuations in terms of a transient fractional diffusion equation. This description allows us to take into account the presence of a distribution of time scales, with a power law decay of the

dx.doi.org/10.1021/jp412125d | J. Phys. Chem. B 2014, 118, 3823−3831

correlation function at intermediate times and asymptotic exponential decay.

One of the main interests of this approach is its ability to take into account a continuous distribution of time scales, rather than a single one as in the usual case of jump processes, while keeping the number of model parameters constant and relatively low. Our analysis of the chemical shift trajectories obtained from MD simulations probing two dramatically different time scales showed the multiscale, fractional, character of the resonance frequency fluctuations, thus providing an alternative view of the stochastic processes underlying the associated NMR exchange rate. These results further support the fractional character of the diffusive processes that was previously identified in protein internal dynamics.[34,35]

APPENDIX: JUSTIFICATION FOR A TRANSIENTLY FRACTIONAL STOCHASTIC PROCESS

In this Appendix, we propose a justification of the variable order fractional differential equation eq 11 for the description of the transient fractional diffusion model used in this work. In the CTRW model of diffusion, the diffusing particle jumps between nodes located on a grid, where it sits for a random waiting time t characterized by a probability distribution function $\psi(t)$ that decreases as[19,36]

$$\psi(t) \sim (t/\zeta)^{-(\alpha+1)} \qquad \text{for} \qquad t \to \infty \tag{28}$$

Alternatively, one has for the moment generating function $\hat{\psi}(s)$, the Laplace transform of $\psi(t)$:

$$\hat{\psi}(s) \sim 1 - (\zeta s)^{\alpha} \qquad \text{for} \qquad s \to 0 \tag{29}$$

When $0 < \alpha < 1$, the first moment of the waiting time probability distribution function diverges, so that $\langle t \rangle = \int_0^\infty t\psi(t)\, dt = \infty$.

To illustrate the idea of a transiently fractional stochastic process, consider the following example:

$$\psi(t) = (\sqrt{1/\zeta_0} + \sqrt{1/\zeta})e^{-t/\zeta_0} \times \left[(\pi t)^{-1/2} - \frac{1}{\sqrt{\zeta}} e^{t/\zeta}\, \mathrm{erfc}(t^{1/2}/\sqrt{\zeta}) \right] \tag{30}$$

Its Laplace transform is given by[46]

$$\psi(s) = \frac{(\sqrt{1/\zeta_0} + \sqrt{1/\zeta})}{\sqrt{s + 1/\zeta_0} + \sqrt{1/\zeta}} \tag{31}$$

Assume that $\zeta_0 \gg \zeta$ and consider the limit of "small" s ($s \ll 1/\zeta_0$). One may approximate $\psi(s)$ as

$$\psi(s) \sim 1 - \frac{\sqrt{\zeta\zeta_0}}{2} s \tag{32}$$

This corresponds to normal diffusion, which was expected from the exponential pre-factor in eq 30. Alternatively, in the case where $0 \ll 1/\zeta_0 \ll s \ll 1/\zeta$:

$$\psi(s) \approx 1 - (\zeta s)^{1/2} + \ldots \tag{33}$$

which describes fractional diffusion with $\alpha = 1/2$. Thus, in this exactly tractable example, the waiting time pdf $\psi(t)$ decays as $(t/\zeta)^{-3/2}$ for $\zeta \ll t \ll \zeta_0$, characteristic of fractional diffusion. Alternatively, $\psi(t) \sim (2t/(\zeta\zeta_0)^{1/2})^{-2}$ for $t \gg \zeta_0$, the signature of normal diffusion, as $t \to \infty$.

One can construct a process for which the waiting time pdf obeys approximate expressions of the type given in eqs 28 and 29 with different values (α, ζ) and $(1, \zeta_0)$ for the respective time intervals $\zeta_0 \gg t \gg \zeta$ and $t \gg \zeta_0$. Diffusion can therefore be modeled by fractional diffusion equations with parameter $\alpha_i = \alpha$ and scaling factor $\tau_i = \tau_0$ in the interval $\zeta_0 \gg t \gg \zeta$:

$$\frac{\partial P(x,t)}{\partial t} = \tau_i^{-\alpha_i}\, {}_0\mathcal{D}_t^{1-\alpha_i} L_{\mathrm{FP}} P(x,t) \tag{34}$$

and by normal diffusion $(\alpha_i = 1)$ with $\tau_i = \tau_0$ for $t \gg \zeta_0$. We now assume the possibility for α to continuously vary between α_0 and 1 with time, so that one may thus write a variable order kind of fractional FPE:

$$\frac{\partial P(x,t)}{\partial t} = \tau(t)^{-\alpha(t)}\, {}_0\mathcal{D}_t^{1-\alpha(t)} L_{\mathrm{FP}} P(x,t) \tag{35}$$

A general method of solution of this variable order fractional differential equation where α depends only on the upper limit of the integral is to introduce an auxiliary time variable t_1, so that $\alpha = \alpha(t_1)$ and[18]

$$\frac{\partial P(x,t)}{\partial t} = \tau(t_1)^{1-\alpha(t_1)}\, {}_0\mathcal{D}_t^{1-\alpha(t_1)} L_{\mathrm{FP}} P(x,t) \tag{36}$$

Equation 36 is then doubly Laplace transformed with respect to t and t_1 and solved in the Laplace domain with variables (s, s_1). The solution of the equation is then taken for $t = t_1$ after back-transformation in the time domain. This equation is not in general amenable to an analytical solution.

AUTHOR INFORMATION

Corresponding Authors

*P. Calligari: e-mail, paolo.calligari@sissa.it.

*D. Abergel: e-mail, daniel.abergel@ens.fr.

Notes

The authors declare no competing financial interest.

ACKNOWLEDGMENTS

This work was granted access to the HPC resources of [CCRT/CINES/IDRIS] under the allocation 2011-t2010076423 made by GENCI (Grand Equipement National de Calcul Intensif). P.C. acknowledges the Agence Nationale de la Recherche (ANRContract ANR-COSI-2010-001-01) and the International School for Advanced Studies (NOFYSAS 2012 Grants For Young Researchers) for funding. We thank D. E. Shaw Research for sharing the MD simulation data with the scientific community.

REFERENCES

(1) Henzler-Wildman, K. A.; Lei, M.; Thai, V.; Kerns, S. J.; Karplus, M.; Kern, D. A Hierarchy of Timescales in Protein Dynamics is Linked to Enzyme Catalysis. *Nature* **2007**, *450*, 913−916.

(2) Daniel, R.; Dunn, R.; Finney, J.; Smith, J. The Role of Dynamics in Enzyme Activity. *Annu. Rev. Biophys. Biomol. Struct.* **2003**, *32*, 69−92.

(3) Hammes, G. G. How do Enzymes Really Work? *J. Biol. Chem.* **2008**, *283*, 22337−22346.

(4) Jarymowycz, V.; Stone, M. Fast Time Scale Dynamics of Protein Backbones: NMR Relaxation Methods, Applications, and Functional Consequences. *Chem. Rev.* **2006**, *106*, 1624−1671.

(5) Kay, L. E. NMR Studies of Protein Structure and Dynamics. *J. Magn. Reson.* **2005**, *173*, 193−207.

(6) Boehr, D. D.; Dyson, H. J.; Wright, P. E. An NMR Perspective on Enzyme Dynamics. *Chem Rev* **2006**, *106*, 3055−3079.

(7) Robustelli, P.; Stafford, K. A.; Palmer, A. G., 3rd. Interpreting Protein Structural Dynamics from NMR Chemical Shifts. *J. Am. Chem. Soc.* **2012**, *134*, 6365−6374.
(8) Wishart, D.; Watson, M.; Boyko, R.; Sykes, B. Automated 1H and 13C Chemical Shift Prediction Using the BioMagResBank. *J. Biomol. NMR* **1997**, *10*, 329−336.
(9) Shen, Y.; Bax, A. Protein Backbone Chemical Shifts Predicted from Searching a Database for Torsion Angle and Sequence Homology. *J. Biomol. NMR* **2007**, *38*, 289−302.
(10) Shen, Y.; Bax, A. SPARTA+: a Modest Improvement in Empirical NMR Chemical Shift Prediction by Means of an Artificial Neural Network. *J. Biomol. NMR* **2010**, *48*, 13−22.
(11) Han, B.; Liu, Y.; Ginzinger, S. W.; Wishart, D. S. SHIFTX2: Significantly Improved Protein Chemical Shift Prediction. *J. Biomol. NMR* **2011**, *50*, 43−57.
(12) Xu, X.; Case, D. A. Automated Prediction of 15N, 13Cα, 13Cβ and 13C′ Chemical Shifts in Proteins Using a Density Functional Database. *J. Biomol. NMR* **2001**, *21*, 321−333.
(13) Moon, S.; Case, D. A New Model for Chemical Shifts of Amide Hydrogens in Proteins. *J. Biomol. NMR* **2007**, *38*, 139−150.
(14) Kohlhoff, K. J.; Robustelli, P.; Cavalli, A.; Salvatella, X.; Vendruscolo, M. Fast and Accurate Predictions of Protein NMR Chemical Shifts from Interatomic Distances. *J. Am. Chem. Soc.* **2009**, *131*, 13894−13895.
(15) Shaw, D.; Deneroff, M.; Dror, R.; Kuskin, J.; Larson, R.; Salmon, J.; Young, C.; Batson, B.; Bowers, K.; Chao, J.; et al. Anton, a special-purpose machine for molecular dynamics simulation. *Commun. ACM* **2008**, *51*, 91−97.
(16) Shaw, D. E.; Maragakis, P.; Lindorff-Larsen, K.; Piana, S.; Dror, R. O.; Eastwood, M. P.; Bank, J. A.; Jumper, J. M.; Salmon1, J. K.; Shan1, Y.; et al. Atomic-Level Characterization of the Structural Dynamics of Proteins. *Science* **2010**, *330*, 341−346.
(17) Xue, Y.; Ward, J. M.; Yuwen, T.; Podkorytov, I. S.; Skrynnikov, N. R. Microsecond Time-Scale Conformational Exchange in Proteins: Using Long Molecular Dynamics Trajectory To Simulate NMR Relaxation Dispersion Data. *J. Am. Chem. Soc.* **2012**, *134*, 2555−2562.
(18) Lorenzo, C. F.; Hartley, T. T. Variable Fractional Order and Distributed Order Operators. *Nonlinear Dyn.* **2002**, *29*, 57−98.
(19) Metzler, R.; Klafter, J. The Random Walk's Guide to Anomalous Diffusion: A Fractional Dynamics Approach. *Phys. Rep.* **2000**, *339*, 1−77.
(20) Lindorff-Larsen, K.; Piana, S.; Palmo, K.; Maragakis, P.; Klepeis, J. L.; Dror, R. O.; Shaw, D. E. Improved Side-Chain Torsion Potentials for the Amber ff99SB Protein Force Field. *Proteins* **2010**, *78*, 1950−1958.
(21) Horn, H. W.; Swope, W. C.; Pitera, J. W.; Madura, J. D.; Dick, T. J.; Hura, G. L.; Head-Gordon, T. Development of an Improved Four-site Water Bodel for Biomolecular Simulations: TIP4P-Ew. *J. Chem. Phys.* **2004**, *120*, 9665−9678.
(22) Bussi, G.; Donadio, D.; Parrinello, M. Canonical Sampling through Velocity Rescaling. *J. Chem. Phys.* **2007**, *126*, 014101.
(23) Parrinello, M.; Rahman, A. Polymorphic Transitions in Single Crystals: A New Molecular Dynamics Method. *J. Appl. Phys.* **1981**, *52*, 7182−7190.
(24) Calandrini, V.; Pellegrini, E.; Calligari, P.; Hinsen, K.; Kneller, G. nMoldyn - Interfacing Sepectroscopic Experiments, Molecular Dynamics Simulations and Models for Time Correlation Functions. *Collection SFN* **2011**, *12*, 201−232.
(25) Byrd, R. H.; Lu, P.; Nocedal, J.; Zhu, C. A Limited Memory Algorithm for Bound Constrained Optimization. *SIAM Journal of Scientific Computing* **1995**, *16*, 1190−1208.
(26) Abragam, A. *Principles of Nuclear Magnetism*; Clarendon Press: Oxford, U.K., 1961.
(27) Schurr, J. M.; Fujimoto, B. S.; Diaz, R.; Robinson, B. H. Manifestations of Slow Site Exchange Processes in Solution NMR: A Continuous Gaussian Exchange Model. *J. Magn. Reson.* **1999**, *140*, 404−431.
(28) Shlesinger, M. F.; Montroll, E. W. On the Williams−Watts Function of Dielectric Relaxation. *Proc. Natl. Acad. Sci. U. S. A.* **1984**, *81*, 1280−1283.
(29) Barkai, E.; Metzler, R.; Klafter, J. From Continuous Time Random Walks to the Fractional Fokker-Planck Equation. *Phys. Rev. E* **2000**, *61*, 132−138.
(30) Glöckle, W.; Nonnenmacher, T. A Fractional Calculus Approach to Self-similar Protein Dynamics. *Biophys. J.* **1995**, *68*, 46−53.
(31) Lu, H.; Xun, L.; Xie, X. S. Single-Molecule Enzymatic Dynamics. *Science* **1998**, *282*, 1877−1882.
(32) Kneller, G.; Hinsen, K. Fractional Brownian Dynamics in Proteins. *J. Chem. Phys.* **2004**, *121*, 10278−10283.
(33) Calandrini, V.; Abergel, D.; Kneller, G. Fractional Protein Dynamics Seen by Nuclear Magnetic Resonance Spectroscopy: Relating Molecular Dynamics Simulation and Experiment. *J. Chem. Phys.* **2010**, *133*, 145101.
(34) Calligari, P.; Calandrini, V.; Kneller, G. R.; Abergel, D. From NMR Relaxation to Fractional Brownian Dynamics in Proteins: Results from a Virtual Experiment. *J. Phys. Chem. B* **2011**, *115*, 12370−12379.
(35) Calligari, P.; Abergel, D. Toward the Characterization of Fractional Stochastic Processes Underlying Methyl Dynamics in Proteins. *J. Phys. Chem. B* **2012**, *116*, 12955−12965.
(36) Metzler, R.; Barkai, E.; Klafter, J. Anomalous Diffusion and Relaxation Close to Thermal Equlibrium: A Fractional Fokker-Planck Equation Approach. *Phys. Rev. Lett.* **1999**, *82*, 3563−3567.
(37) Oldham, K. B.; Spanier, J. *Theory and Applications of Differentiation and Integration at Arbitrary Order*; Dover: New York, 1974.
(38) Erdélyi, A.; Magnus, W.; Oberhettinger, F.; Tricomi, F. *Higher Transcendental Functions*; McGraw Hill: New York, 1955.
(39) Kneller, G. Quasielastic Neutron Scattering and Relaxation Processes in Proteins: Analytical and Simulation-based Models. *Phys. Chem. Chem. Phys.* **2005**, *7*, 2641−2655.
(40) Calandrini, V.; Abergel, D.; Kneller, G. Protein Dynamics from NMR Perspective: Network of Coupled Rotators and Fractional Brownian Dynamics. *J .Chem. Phys.* **2008**, *128*, 145102.
(41) Mathai, A.; Haubold, H. J. *Special Functions for Applied Scientists*; Springer: NewYork, 2008.
(42) Gorenflo, R.; Loutchko, J.; Luchko, Y. Computation of the Mittag-Leflier Function $E_{\alpha,\beta}$; and its Derivative. *Fractional Calculus and Applied Analysis* **2002**, *5*, 491−518.
(43) Zwanzig, R.; Ailawadi, N. K. Statistical Error Due to Finite Time Averaging in Computer Experiments. *Phys. Rev.* **1969**, *182*, 280−283.
(44) Grey, M. J.; Wang, C. Y.; Palmer, A. G. Disulfide Bond Isomerization in Basic Pancreatic Trypsin Inhibitor: Multisite Chemical Exchange Quantified by CPMG Relaxation Dispersion and Chemical Shift Modeling. *J. Am. Chem. Soc.* **2003**, *125*, 14324−14335.
(45) Loria, J. P.; Rance, M.; Palmer, A. G. A TROSY CPMG Sequence for Characterizing Chemical Exchange in Large Proteins. *Methods Enzymol.* **2001**, *339*, 204−238.
(46) Schiff, J. L. *The Laplace Transform: Theory and Applications*; Springer: NewYork, 1999.